CARBON FIBER COMPOSITE B-PILLAR REINFORCEMENT MANUFACTURING: PLY NESTING AND AUTOMATED PLY LAYUP

Matthew Rebandt, Jeff Dahl, Michael Cacovic

Ford Motor Company

Abstract

To reduce vehicle mass and increase fuel efficiency, carbon fiber composites are being considered for structural body components. As a demonstrator, a B-Pillar reinforcement was designed with continuous carbon fiber prepreg as the material system. Based upon structural analysis and subsequent ply layup determination, a tri-axial non-crimped fabric (NCF) was selected as the base fiber architecture so achieving a high material utilization was critical for cost effective manufacturing. Two dimensional ply nesting software was used to optimize material utilization and simulate ply cutting time for individual plies. Following ply cutting, automated ply layup is a required processing step for fully automated manufacturing of carbon fiber composites. The experimental effort presented was focused on the ultrasonic welding of thermoset prepregs during automated ply layup. Additionally, predictive models were developed based upon experimental data and will be presented.

Background and Requirements

Carbon fiber prepreg can be manufactured using a variety of fabric architectures including braided, woven and non-crimped fabrics (NCF) along with unstitched or stitched unidirectional fibers. In general terms, each fabric architecture type will yield equivalent structural performance in the composite. However, each fabric type will exhibit different characteristics throughout the manufacturing process which must be taken into consideration.

To investigate the applicability of continuous carbon fiber composites in a structural application, a B-Pillar reinforcement was designed. Structural analysis of the B-pillar under side impact and roof crush loads was conducted and the ply layup was determined to be $[(0,60,-60)_{ncf}/(-60,60,0)_{ncf}]_3$ It was then necessary to perform a manufacturing feasibility study on the fabric architecture relative to two dimensional ply cutting. The main areas of interest in this step of the manufacturing process are material utilization and ply cutting cycle time for input to cost modeling activities. Material cost is generally the largest component of the overall cost when using carbon fiber composites. Hence, maximizing material utilization is paramount. To optimize material utilization, AGFM's NS2 nesting software [1] was used to generate two dimensional ply nests and the resultant ply cutting times. An American GFM CM10 Dynamic machine was selected to be used for the study, because it has a lower capital cost, and higher cutting speed when compared to their other machines.

For implementation of carbon fiber composites in automated manufacturing, methods are required and processing parameters must be well defined for repeatable and robust processes. Automated ply layup is one processing step for fully automated manufacturing of carbon fiber composites. The cell used consists of nesting tables for ply placement, an ultrasonic welding unit to weld prepreg plies together in the desired ply layup and a robot for required pick and place operations. Welding of thermoset prepreg plies is an enabler for automated robotic handling of ply layups.

Nesting Simulations

The two dimensional geometry of the carbon fiber composite B-pillar reinforcement is determined from the three dimensional model. The three dimension model is imported into Siemens Fibersim software to create the two dimensional blank geometries based upon material type via the forming simulation. To optimize material utilization, AGFM's NS2 nesting software was used to generate two dimensional ply nests and the resultant ply cutting times.

Figure 1: American GFM ultra sonic cutter CM10 machine, used to cut composite prepreg.

Because of the fiber architectures under consideration, the tri-axial NCF is required as three plies contained within the NCF (-60/0/60). The two 0° plies specified $[-60/0_2/60]_{2s}$ are combined into one ply of twice the areal mass to minimize complexity. Since off-axis fibers are contained within the NCF, only one ply blank type is required. In order to create a symmetric laminate, however, two different rolls of material are required (-60/0/60 and 60/0/-60).

In order to form and trim the part in a repeatable fashion, the original blank geometry obtained via Fibersim was increased. The increase in size is required to hold the blank during forming, thereby preventing wrinkling or over stretching the fiber and ensuring that the entire perimeter is beyond the edge of part. The additional material is trimmed during preforming process creating a net shape component for compression molding.

The additional material also allows the expanded blank geometry profile to be optimized to increase cutting speed and reduce cycle time. Tight radii, corners and rough lines were modified to create smooth tangent transitions along the cutting path. This also allowed for a continuous path versus having to start and stop and move the head up and down to start new cuts. By eliminating unnecessary movements, the cutting time was decreased from 73.2 seconds to 5.4 seconds a ply, improving the cutting cycle time 1,356.6%. With these changes the cutting length was unaffected and the surface area was increased by less than 0.01%.

The modified, two dimensional ply was imported into the NS2 Nesting System [1] software to optimize material utilization and determine ply cutting cycle time. Fiber orientation, the number of plies required, roll width, machine type and the size of the cutting machine were all accounted for within the software. With these constraints, the software optimized material utilization and provided an estimated cutting cycle time based upon the cutting machine kinematics. Due to the fiber angles specified in the ply layup and the NCF architecture, only a 180° rotation of the plies could be performed during nesting to improve utilization while

maintaining the specified fiber orientations in the B-Pillar reinforcement.

The CM10 Dynamic ply cutting machine featured an automated material unrolling system that feeds material off of the roll and into the cutting window. After material in the cutting table window was cut, the conveyor dispensed additional material into the cutting window. The conveyorized material dispensing system moves at 115 mm/s. This transfer rate was applied to each material nest to determine the time for each length of material required to be unrolled. The reported ply cutting time was the time for the ply to be cut plus the time for the conveyor to unroll the material.

Carbon fiber NCF materials and subsequent prepregs both have width limitations based upon existing manufacturing equipment. NCF manufacturing is typically limited to 2540 mm wide based on supply base capabilities. Additionally, prepreg manufacture is typically limited to 1500 mm. Because of the different constraints, a NCF fabric can be manufactured larger than the prepreg limitations and then slit prior to winding. This allows twice the fabric throughput from the same machine; hence, this option was examined as it will affect overall manufacturing costs. Two different roll widths were then considered for nesting studies. The first having a fabric that is slit before prepregging and the second being a material limited by the prepregging process.

Due to the geometry of the B-pillar preform when nested, it has a higher utilization when paired together along the width of the material and alternating in direction by 180°. To achieve the highest utilization, the plies were nested as an even number across the width. The maximum widths for the NCF are 1270 mm for the slit roll or 1500 mm for prepreg manufacturing. With these limiting dimensions, a maximum of four (4) plies could be nested across a 1270 mm roll, whereas a maximum of six (6) plies could be nested across a 1500 mm roll. A partial nest example for the four ply width assumption is given in Figure 2. Using these constraints, nesting simulations to determine the highest possible material utilization were conducted.

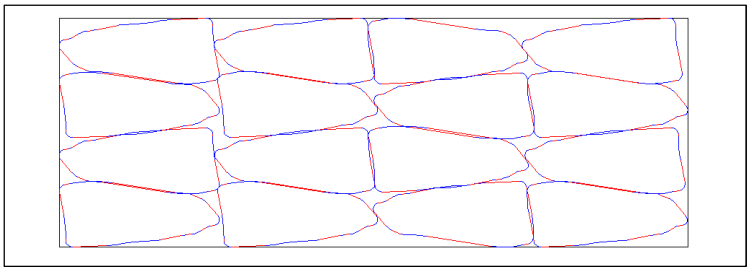

Figure 2: Nest of b-pillar with 4 plies across.

Results

Four Ply Width Nest Scenario

In the four ply width nest scenario shown in Figure 2, five different nest sizes were investigated (4, 8, 12, 16 and 20 plies) with each nest being a multiple of the original four ply width assumption. The highest material utilization for the four (4) ply nest was at a roll width of 997 mm. The highest utilization for the eight (8) and 12 ply nests was with a 1008 mm wide roll. For both the 16 and 20 ply nests, the highest material utilization was achieved with a roll width of 999 mm. The 20 ply nest at a roll width of 999 mm yielded the highest material utilization of 87.2%.

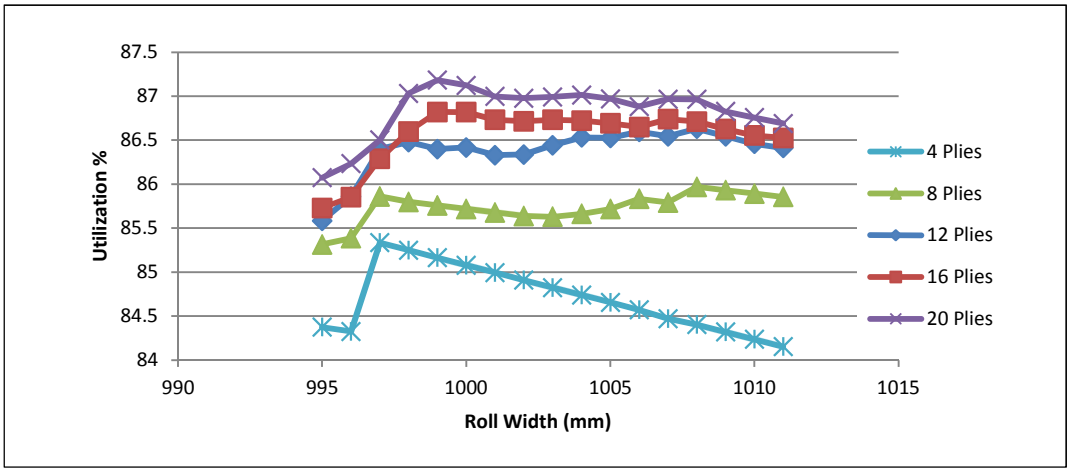

Figure 3: Material utilization versus roll width, four ply width nest scenario

Not surprisingly, material utilization was increased with an increased number of plies in the nest. Examining the 16 and 20 ply nests, material utilization increased from 86.8 to 87.2% with only four additional plies. It is then obvious that nests containing more plies should be examined to determine the effect on material utilization. However, execution time for the analysis increased with the ply count, due to limited software and computing and the 20 ply nest was the largest that was analyzed. An optimum nest to yield the highest material utilization at a roll length of 150 meters could not be determined.

Six Ply Width Nest Scenario

For the six ply width nest scenario, three different nest sizes were investigated (6, 12 and 18 plies) with each nest being a multiple of the original six ply width assumption. The highest material utilization of 88.1% was achieved at a roll width of 1482 mm. As expected, this was achieved with the largest nest, the 18 ply nest. In this instance, material utilization increased by 0.6% when increasing the nest size from 12 to 18 plies. Again, software and computing power limited the maximum nest size to 18 plies.

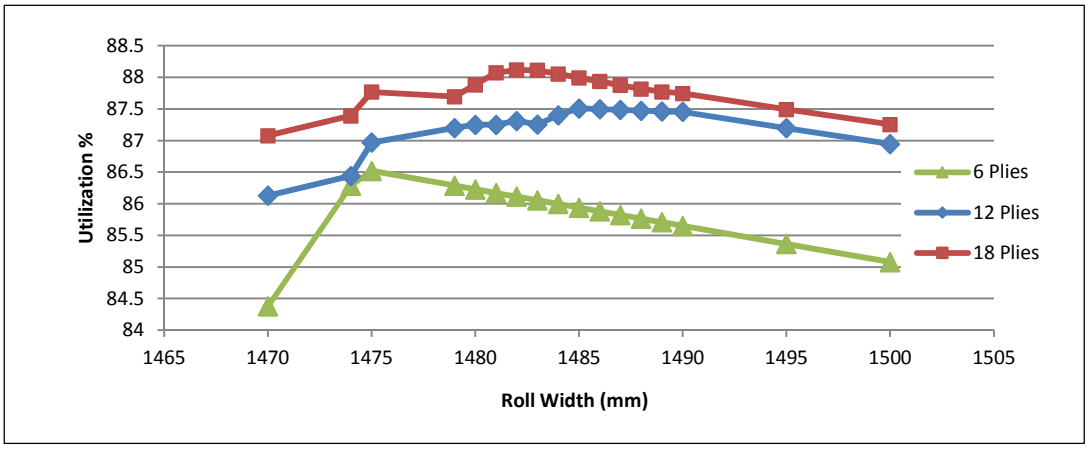

Figure 4: Material utilization versus roll width, six ply width nest scenario.

Long Nest Computing Issues

Due to limitations of computer processing, an optimum nest to yield the highest material utilization at a roll length of 150 meters could not be determined. To be sure, repeated attempts

to analyze a 24 ply nest in the four ply width nest scenario returned material utilization values lower than the 20 ply nest. This was despite an additional 13 hours of computational time (5 versus 18 hours). Similar issues were encountered with the six ply width nests.

Four Ply Width, Long Nest Scenario

Three different four ply wide nests were used to determine material utilization off of a 150 meter long roll. These were a 16 ply nest, a 20 ply nest and also a 16 ply nest created from the 20 ply nest. In the last instance, the last four plies were removed from the 20 ply nest to create another alternative. This was done to generate a 16 ply nest which could be rotated 180° thereby creating a different nest pattern and more options for optimizing material utilization. Material utilization versus roll width data for the three ply nests examined are graphically displayed in Figure 5.

A long nest of the 16 ply nest generated from the 20 ply nest yielded the highest material utilization at 88.1%. The roll width was 999 mm. This result is 0.9% higher than the utilization determined for a single 20 ply nest in the first analysis. Both long nests from the 16 and 20 ply nests yielded slightly lower material utilization at 87.4 and 87.9%, respectively. It is believed that this is due to the rotational ability of the 16 ply nest generated from the 20 ply nest to create a different pattern. In the case of the other two nests examined, a 180° rotation created the same nest.

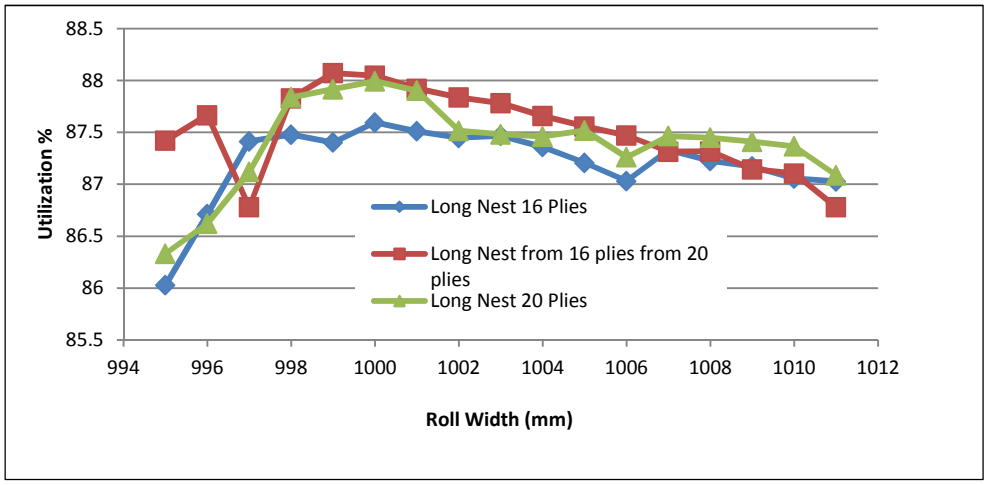

Figure 5: Four ply width long nest results, utilization versus roll width, roll length of 150 meters

Six Ply Width, Long Nest Scenario

The previously developed 12 and 18 ply nests were nested to a maximum length of 150 meters at various roll widths (Figure 6) to determine the maximum material utilization. The 12 ply nest yielded a higher material utilization than the 18 ply nest at 89.1 versus 88.9% both at a roll width of 1480 mm. This was a 1.0% increase in material utilization versus the single 18 ply nest results. As seen in the four ply width long nest results, this was more than likely due to the fact that the 12 ply nest can be rotated 180° creating a different pattern. This allowed for more nesting options to increase density and thus utilization. In the case of the 18 ply nest, the nest was the same when rotated allowing for fewer nesting options. The rotational capability was evident by examining both ply nests.

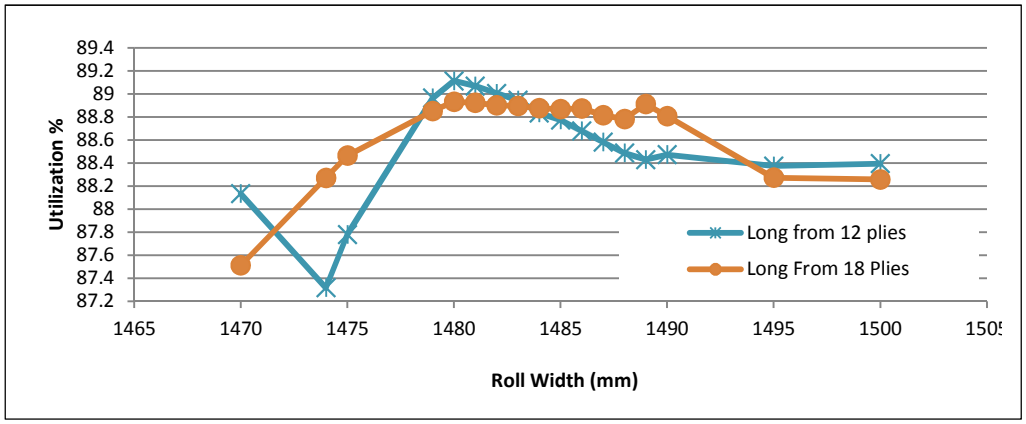

Figure 6: Six ply width long nest results, utilization versus roll width, roll length of 150 meters

Data Summary

The analysis results for both ply width scenarios are summarized in Table I. To accommodate the tolerance of the automated edge guiding system as well as the profiling tolerance of the cutting machine, an additional 10 mm was added to the optimum material width. This reduced material utilization determined via the nesting software but the extra width cannot be included as it would affect the nesting. The preform ply utilization was the two dimensional utilization directly from the roll.

With a four ply width nest, the highest material utilization of 87.2% was found at a roll width of 1009 mm. The cycle time per part was 44.8 seconds. With a six ply width nest, the highest material utilization of 88.5% was found at a roll width of 1490 mm and the cycle time per part was 41.6 seconds. The optimum six ply width nest yielded a 1.3% improvement in material utilization and a 3.2 second per part cycle time improvement versus the optimum four ply width nest.

Table I: Four plies wide vs six plies wide prepreg

	4 ply width		6 ply width	
	Short Nest	Long Nest	Short Nest	Long Nest
Roll width (mm)	1009	1009	1492	1490
Length (mm)	3427	149286	2057	149388
Preform ply utilization (%)	86.3	87.2	87.5	88.5
Time per ply (s)	7.6	7.5	7.1	6.9
Time per part (s)	45.8	44.8	42.6	41.6

Ultrasonic Welding Development

Manufacturing viability of a high volume automated system will include successful development of cutting, blank handling, ply layup with ultrasonic stitching, preforming, and molding of a carbon fiber composite material system. The thrust area detailed below is for ultrasonic stitching of a carbon fiber thermosetting resin prepreg system. The development of an ultrasonic stitching process has two prime objectives; to develop ultrasonic stitching process parameters that will exhibit sufficient strength for automated handling of the ply layups and to develop and optimize ultrasonic welding parameters for ply layup configurations that will produce stitching capabilities with no horn interface sticking and no advancement in the resin material cure kinetics.

For successful implementation of carbon fiber composites in automotive components, automated manufacturing methods are required and processing parameters must be well defined for repeatable and robust processes. Figure 7, shows an automated manufacturing cell for carbon fiber composites. The cell consists of nesting tables for ply placement, an ultrasonic welding unit to weld prepreg plies together and a robot for required pick and place operations.

This work expands on previous efforts that scoped down and narrowed in on the ultrasonic inputs and parameters by incorporating a quantitative measurement of weld strength and predictive models based upon experimental results. Additionally, the effect of process variables on weld energy was also explored. The results generated will be used to further optimize the ultrasonic welding of thermoset prepregs to achieve welds suitable for automated robotic handling of ply layups.

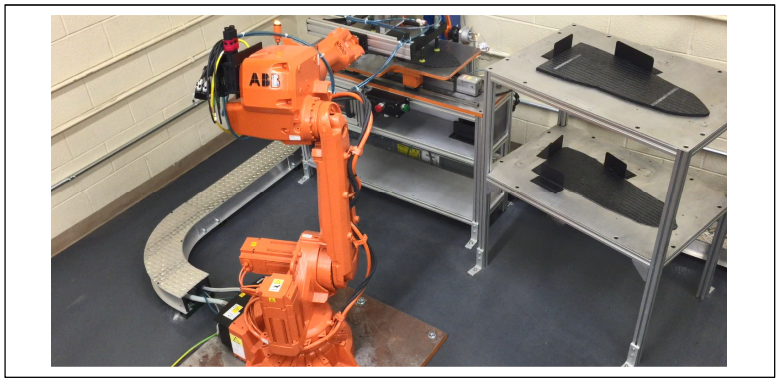

Figure 7: Automation cell performing pick and place operation, onto an ultrasonic unit.

An ultrasonic stitch machine was designed with an acoustic titanium horn to ultrasonically stich the prepreg plies for a specified ply layup. The power supply transfers a high fequency vibrational energy from the horn to the thermosetting prepreg on contact. The energy induced from the ultrasonic system is converted to heat through friction, which tacks the prepreg layers together and forms a stitch to create the ply layup stack. The unit implemented to demonstrate prepreg stitching was the Branson model 2000Xeat20:40.0.

The material system used for ultrasonic welding trials was a thermosetting carbon fiber prepreg, consisting of Dow P6300 prepreg material (2x2 Twill). Weld strength characterization was conducted using ASTM D5868 [3] as a guideline. Due to the horn size, standard lap shear specimens were not feasible and fabric grippers caused buckling and misalignment of the specimens when loaded. A new test fixture was designed, fabricated, and assembled to perform the tests on to eliminate these issues. Prepreg samples were cut to size and a two-layer weld was performed accordingly.

Results

A designed experiment, was developed to examine four factors when welding thermoset prepregs (Table II). Hold time was held constant at two seconds. Weld strength and energy were examined as experimental responses. For each experimental run, a total of 5 specimens were tested and sample means calculated for data analysis. All significance testing was performed at the 95% confidence interval.

Table II: 2-level, full factorial

Factor	-	+
Amplitude (%)	30	40
Weld Time (s)	0.4	0.7
Weld Air Pressure (psi)	30	100
Trigger Pressure (psi)	1	25

The main and interaction effects plots for weld strength are given in Figures 8 and 9. All four factors were determined to be significant with respect to weld strength. Weld time and amplitude had the largest effect with respect to weld shear strength. With a high weld time setting, the mean shear strength was 3.0 kN whereas with a low weld time setting the mean shear strength was 1.5 kN. Amplitude was nearly as significant with weld strengths of 2.9 versus 1.6 kN for the high and low data means, respectively. The effect of air pressure and trigger pressure, although statistically significant, was much less than weld time or amplitude which is clearly evident from the main effects plot. Three, two-way interactions were also determined to be significant with respect to weld strength. Trigger pressure-air pressure was found to be the most significant two way interaction and that of weld time-amplitude and amplitude-trigger pressure being the least significant.

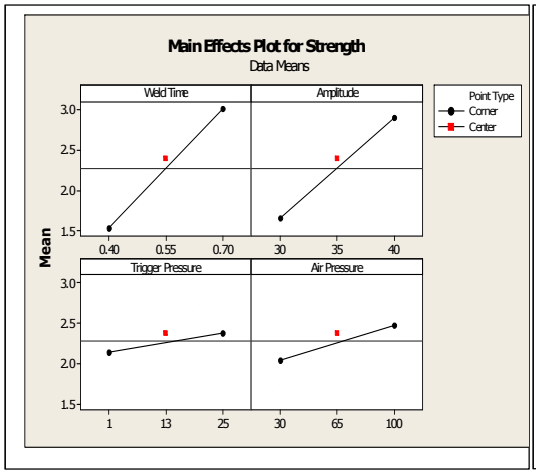

Figure 8: Main effects plot, weld strength

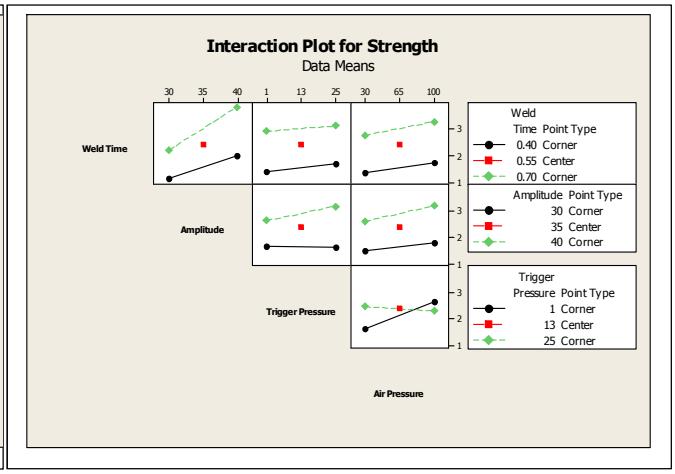

Figure 9: Interaction effects plot, weld strength

The main and interaction effects plots for weld energy are given in Figures 10 and 11. As with weld strength, all four main factors were determined to be significant with respect to weld energy. Weld time and amplitude were the most significant with differences between the data means of 425 and 310 J, respectively. The two way interactions of weld time-amplitude and trigger pressure-air pressure were also found to be significant. An analysis of variance determined that 95% of variation could be attributed to the main effects and 4% to the two way interactions with the remainder being residual error.

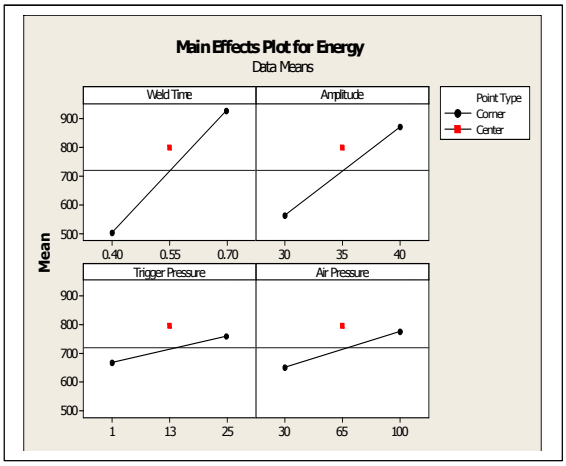

Figure 10: Main effects plot, weld energy

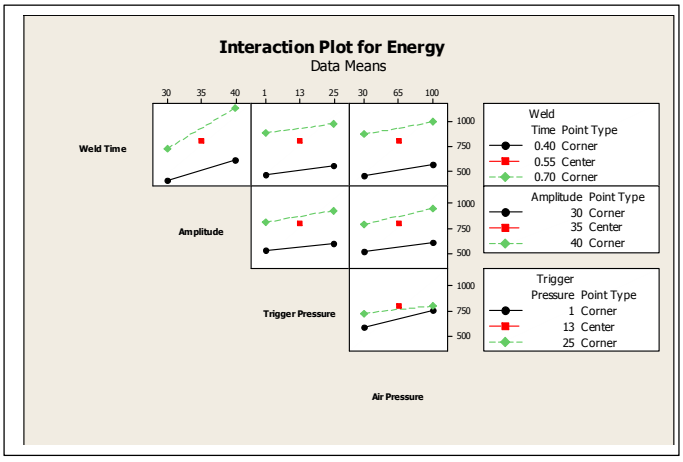

Figure 11: Interaction effects plot, weld energy

Subsequent to the above analysis it was indicated by the manufacture that the downspeed of the horn affected the rate of force build up on the prepreg. It was believed that this could affect energy transfer to the material and subsequently weld strength. To investigate this, an experiment was conducted, was a 2-level factorial at a half fraction design as shown in Table III. Parameters for the previous four factors were not altered and hold time was held constant at two seconds. Again, both weld strength and weld energy were analyzed as experimental responses. Five specimens were tested for each run to determine weld strength. All significance testing was performed at the 95% confidence interval.

Table III: 2-level factorial, ½ fraction design

Factor	**-**	**+**
Amplitude (%)	30	40
Weld Time (s)	0.4	0.7
Weld Air Pressure (psi)	30	100
Trigger Pressure (psi)	1	25
Downspeed	25	100

All five factors were determined to be significant with respect to weld shear strength. Again, weld time and amplitude had the largest effect as evidenced in Figure 12. Trigger pressure and air pressure were again significant, albeit at a lower level than weld time and amplitude. As for downspeed, the slope for the data means was the smallest and least significant with regard to strength for both the main and interaction effects.

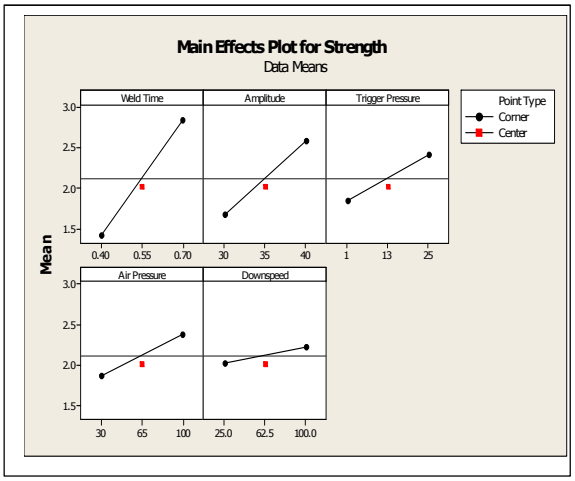

Figure 12: Main effects plot, weld strength

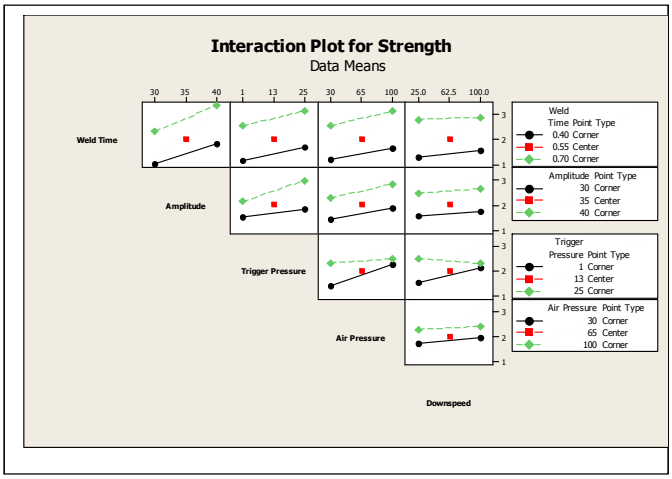

Figure 13: Interaction effects plot, weld strength

Three, two way interaction effects were determined to be significant as well. Trigger pressure-downspeed was the most significant two way interaction. Trigger pressure-air pressure and amplitude-trigger pressure were determined to have slightly less effect (Figures 13 and 14).

These significant effects are different than those relative to weld strength. This can be attributed to the addition of downspeed as a factor as both downspeed and the interaction of trigger pressure-downspeed were determined to be significant (Figure 14). Based upon the experimental data, a predictive model for weld strength was developed. The R^2-(adj) value was found to be 97.91% indicating good agreement between the model and experimental data. The R^2-(pred) value was 94.93% suggesting reasonable predictive capability within the experimental bounds.

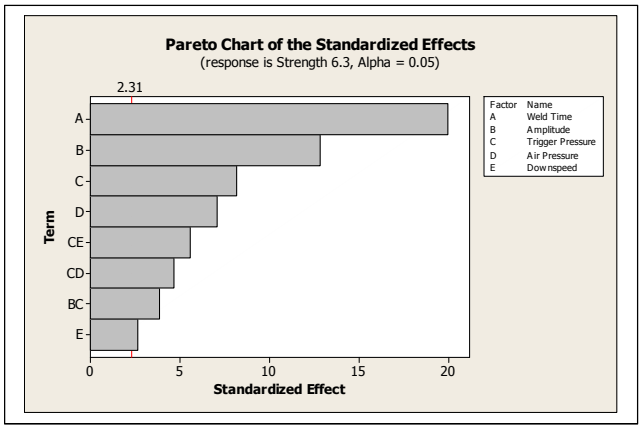

Figure 14: Pareto chart of significant effects, weld strength

The main and interaction effects plots for weld energy are given in Figures 15 and 16. Four of the five main factors were determined to have a significant effect on weld energy with downspeed being the only insignificant factor. As in the previous experiment, weld time and amplitude had the most significant effect with both trigger pressure and air pressure being less significant (Figure 14). The two way interactions of weld time-amplitude and trigger pressure-air pressure were also found to be significant.

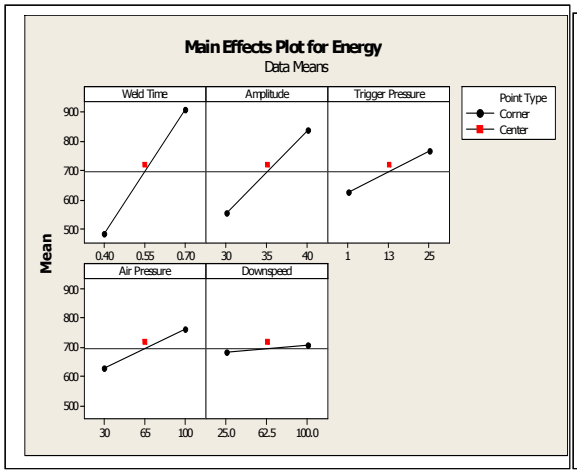

Figure 15: Main effects plot, weld energy

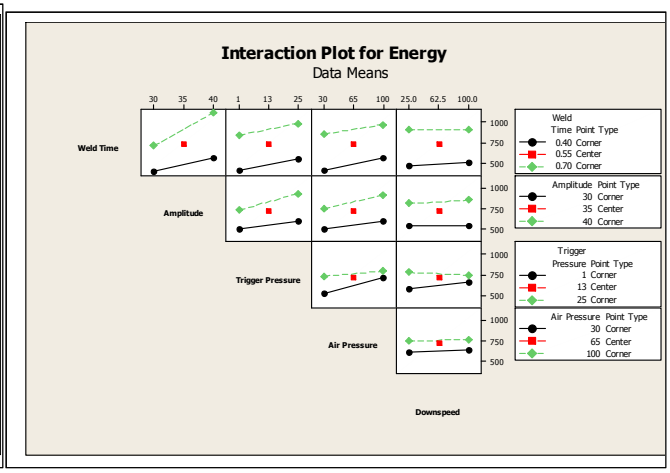

Figure 16: Interaction effects plot, weld energy

An analysis of variance determined that 92% of variation could be attributed to the main effects and 6% to the two way interactions with the remainder being residual error. These results are consistent with the other findings, despite the addition of downspeed as an experimental factor. With a R^2-(adj) value of 95.74%, the model fits well to the experimental data. However, the R^2-(pred) value was 91.77% indicating reasonable predictive capability within the experimental space. It is believed that completion of this experiment from a half fraction to full fraction factorial could improve the model and thus the predictive capability by generating data for the entire design space.

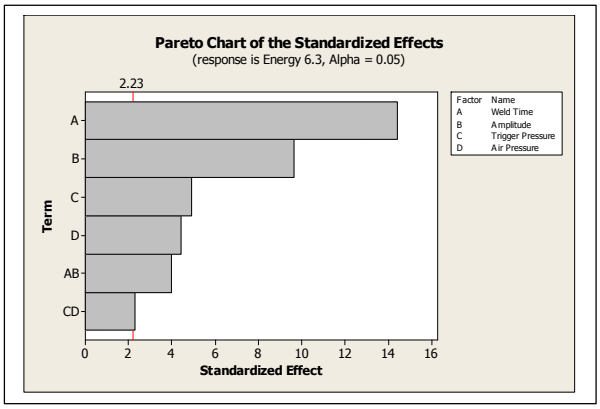

Figure 17: Pareto chart of significant effects, weld energy

Differential Scanning Calorimetry

It is essential that all local ultrasonic welds do not induce any epoxy resin curing. Differential Scanning Calorimetry (DSC) tests were run with a virgin epoxy resin system, epoxy with an ultrasonic weld energy of 200 J, and epoxy with an ultrasonic weld energy of 2000 J. To understand the response of the cure kinetics within the prepreg system, it was ideal to measure the minimum and maximum energy bounds within the ultrasonic process. All three resin tests outputted an enthalpy value of 57 J/g. In summary, no resin curing was recognized on the ultrasonically stitched prepreg plies.

Summary and Next Steps

Two dimensional ply nesting software was used to optimize material utilization and simulate ply cutting time for individual plies, thereby determining the most efficient manufacturing options. Optimal roll widths were established upon both fabric and prepreg manufacturing constraints. Based upon the trimmed ply utilization data, opportunities exist to further improve material utilization if the additional material required for preforming can be reduced.

Although an optimum roll width yielding the highest material utilization and shortest cycle time per ply was determined via two dimensional nesting analyses, this may not be the most cost effective solution for the complete component. As these results contain certain upstream and downstream manufacturing assumptions, the cost of other processes including fabric manufacture and prepregging may be affected. Hence, both scenarios must be examined in the overall cost of the B-Pillar reinforcement.

While a solution was found to alleviate computational limitations which led to increased material utilization, this was not the optimal approach. It was not known if this approach determined the true maximum as a single ply was not used but rather an existing nest containing a given number of plies. Both the rotational ability of a nest or lack thereof seems to further support the concern of obtaining the true maximum. This issue requires further investigation to ensure that maximum material utilization can be achieved when using high cost input materials such as carbon fiber prepreg.

Using thermosetting carbon fiber prepreg materials, designed experiments were conducted to understand the effects of ultrasonic welding input variables on the weld energy and lap shear strength. The weld time and amplitude were determined to be most significant factors with respect to both weld strength and weld energy in both designed experiments. Similarly, trigger pressure and air pressure were found to be significant factors in both experiments with respect to both weld strength and weld energy albeit at lower significance. Downspeed and its interaction with trigger pressure were found to be significant effects with respect to weld strength but not with respect to weld energy. Predictive models were developed for both weld strength and weld energy with good agreement to experimental data and reasonable predictive capability

Ultrasonic welding of thermoset prepregs can be affected by material changes and additional designed experiments must be conducted to validate input parameters for new material formulations. Areal mass differences may alter the output window as energy differences may vary and strength may be compromised due to the prepreg collapse differences. Previous welding experiments were conducted with a 254 x 13 mm horn but the B-Pillar reinforcement plies will require a smaller horn for full contact on the prepreg stack. With this reduced horn size, scaling procedures for the current input parameters must be developed and validated. Along with different prepreg systems and horn size changes, the affect of ply layup must also be investigated. The B-Pillar layup requires additional plies versus the two ply stack seen in the experimentation detailed in this report. Each additional prepreg layer beyond a 2-layer stack may affect the force build-up, collapse depth, and subsequently the weld strength of the completed welded stack.

References

1. *NS2 Nesting System*. Vers. 5.5. Chesapeake Virgina: American GFM Corporation, 2013. Computer software.
2. 2000X EA Power Supply Instruction Manual, EDP 100-412-171, Rev. 10, Branson Ultrasonics Corporation, Danbury, Connecticut.
3. ASTM D5868-01(2014), Standard Test Method for Lap Shear Adhesion for Fiber Reinforced Plastic (FRP) Bonding, ASTM International, West Conshohocken, PA, 2014, www.astm.org